

Channeling of ${}^1\text{H}^+$, ${}^2\text{D}^+$, and ${}^3\text{He}^{++}$ Ions in Germanium: A Diffraction Calculation*

DAVID K. BRICE

Sandia Laboratory, Albuquerque, New Mexico

(Received 10 March 1967)

The channeling properties of ${}^1\text{H}^+$, ${}^2\text{D}^+$, and ${}^3\text{He}^{++}$ ions in germanium have been examined, using a diffraction model for the interaction between the lattice and the channeled ions. The stopping power ($-dE/dx$) and the differential mean-square energy spread ($d\sigma^2/dE$) of the channeling energy spectrum have been calculated for each of the above ions in the energy range 3 to 8 MeV for three incident directions in the lattice. The energy states of the electrons in the lattice are approximated by using a shell model of the lattice atoms. Z electrons per atom are assumed to occupy a rigid, negatively charged shell surrounding an atomic core, where Z is an adjustable parameter in the calculation. An harmonic approximation to the shell-core and shell-shell interactions in the lattice then leads to phononlike excitations in which the shell and atomic core are moving out of phase. This introduces a time-dependent polarization in the lattice which interacts strongly with the incident ions. The lower-energy portion of this excitation spectrum is identified with the plasmon spectrum of the solid, and the known properties of the plasmons are included in the calculation. The parameter Z is adjusted to give agreement between the theoretical and experimental channeling energy losses. No experimental data are presently available for comparison with the calculations for ${}^3\text{He}^{++}$. The results indicate that each of the three directions considered in the calculations can be characterized by a reasonable value of Z , which is expected to be $\gtrsim 4$ depending on the degree to which the valence electrons shielded the inner electrons. For ions incident near the directions indicated these values are $\langle 1, 1, 0 \rangle$, $Z = 5.6 \pm 0.3$; $\langle 1, 1, 1 \rangle$, $Z = 8.6 \pm 0.4$; $\langle 1, 1, 2 \rangle$, $Z = 7.2 \pm 0.3$.

I. INTRODUCTION

THE correlated channeling of particles in crystalline solids was discovered in the machine calculations of Robinson, Holmes, and Oen¹ on the slowing of ions in single-crystal lattices in the energy range 1–10 keV. The effect was subsequently verified by a variety of experimental techniques for both light^{2–13} and heavy^{14,15} ions for energies extending from the keV range up into the MeV range. The converse effect, blocking, in which atoms of the crystal inhibit propagation in certain

directions, has also been observed in the emission of α particles¹⁶ and electrons¹⁷ from single crystals containing radioactive materials. Protons from the (d, p) reaction have also been observed in blocking experiments.¹³

Theoretical studies of the channeling of ionic particles have generally been based on a classical picture of the interaction between particle and lattice^{1,18–20} and have successfully accounted for some of the interesting features which have been observed. Among the features which can be accounted for classically are the energy dependence of the angular distribution of the emergent beam of channeled particles and the energy dependence of the acceptance angle for the channeling of an incident beam. Recent theoretical work²¹ shows that diffraction effects are important, however, in the anomalous transmission of channeled particles even for particle wavelengths which are short compared with the lattice spacing of the crystal. In addition, Chadderton²² has concluded from a study of the channeling patterns of protons in Si that diffraction effects *must* be considered when discussing channeling phenomena.

In neither the classical nor the diffraction studies have energy losses or the stopping power of the lattice for channeled particles been determined except for the low-energy range considered in Ref. 1. In the present

* This work supported by the U.S. Atomic Energy Commission.

¹ M. T. Robinson, D. K. Holmes, and O. E. Oen, *Bull. Am. Phys. Soc.* **7**, 171 (1962); M. T. Robinson and O. E. Oen, *Appl. Phys. Letters* **2**, 30 (1963); *Phys. Rev.* **132**, 2385 (1963).

² R. S. Nelson and M. W. Thompson, *Phil. Mag.* **8**, 1677 (1963); **9**, 1069 (1964).

³ G. Dearnaley, *IEEE Trans. Nucl. Sci.* **NS-11**, 243 (1964).

⁴ W. M. Gibson and T. C. Madden, *Bull. Am. Phys. Soc.* **9**, 493 (1964); T. C. Madden and W. M. Gibson, *IEEE Trans. Nucl. Sci.* **NS-11**, 254 (1964).

⁵ C. Erginsoy, H. E. Wegner, and W. M. Gibson, *Phys. Rev. Letters* **13**, 530 (1964); W. M. Gibson, H. E. Wegner, and C. Erginsoy, *Bull. Am. Phys. Soc.* **10**, 43 (1965).

⁶ M. W. Thompson, *Phys. Rev. Letters* **13**, 756 (1964).

⁷ E. Bøgh, J. A. Davies, and K. O. Nielsen, *Phys. Letters* **12**, 129 (1964).

⁸ W. Brandt, J. M. Khan, D. L. Potter, R. D. Worley, and H. P. Smith, *Phys. Rev. Letters* **14**, 42 (1965).

⁹ J. P. Schiffer and R. E. Holland, *Bull. Am. Phys. Soc.* **10**, 54 (1965).

¹⁰ A. R. Sattler and G. Dearnaley, *Phys. Rev. Letters* **15**, 59 (1965).

¹¹ W. M. Gibson, C. Erginsoy, H. E. Wegner, and B. R. Appleton, *Phys. Rev. Letters* **15**, 347 (1965).

¹² B. R. Appleton, C. Erginsoy, H. E. Wegner, and W. M. Gibson, *Phys. Letters* **19**, 185 (1965).

¹³ D. S. Gemmel and R. E. Holland, *Phys. Rev. Letters* **14**, 945 (1965).

¹⁴ G. R. Piercy, F. Brown, J. A. Davies, and M. McCargo, *Phys. Rev. Letters* **10**, 399 (1963).

¹⁵ S. Datz, T. S. Noggle, and C. D. Moak, *Phys. Rev. Letters* **15**, 254 (1965).

¹⁶ B. Domeij and K. Bjorkvist, *Phys. Letters* **14**, 127 (1965).

¹⁷ G. Astner, I. Bergstrom, B. Gomeij, L. Eriksson, and A. Persson, *Phys. Letters* **14**, 308 (1965).

¹⁸ C. Erginsoy, *Phys. Rev. Letters* **15**, 360 (1965).

¹⁹ J. Lindhard, *Phys. Letters* **12**, 126 (1964); *Kgl. Danske Videnskab. Selskab, Mat. Fys. Medd.* **34**, No. 14 (1965).

²⁰ H. O. Lutz, S. Datz, C. D. Moak, and T. S. Noggle, *Phys. Rev. Letters* **17**, 285 (1966); R. von Jan, *ibid.* **18**, 303 (1967).

²¹ R. E. DeWames, W. F. Hall, and G. W. Lehman, *Bull. Am. Phys. Soc.* **11**, 177 (1966); *Phys. Rev.* **148**, 181 (1966).

²² L. T. Chadderton, *Phys. Letters* **23**, 303 (1966).

paper²³ the energy loss and energy spread of the low-energy-loss component of the channeled particle beam are studied for incident ions in the MeV range using a diffraction picture. The transmission of a particle through the lattice is treated as a series of independent scattering events with particle wave functions before and after each event being plane waves.

The electronic states of the crystal are approximated by using a shell model for the atoms of the lattice. Each atom in the lattice is considered as a heavy, positively charged core (which includes the atomic nucleus and the tightly bound inner electrons) and a negatively charged shell of loosely bound electrons. The various shells and cores of the lattice move independently under the mutual forces which exist between them. A similar model has been used to account for the long-range forces needed to explain the phonon-dispersion curves in a variety of materials, in particular for germanium.²⁴

The primitive unit cell in the germanium lattice consists of four independent masses in the above model, two atomic cores, and two electronic shells. Application of ordinary phonon theory²⁵ in the harmonic approximation will then yield four bands of phononlike excitations. Two of these are the ordinary acoustical- and optical-phonon bands which consist of modes for which an atomic core and its associated shell are moving in phase. The remaining two bands correspond to lattice modes in which the atomic core and its associated shell move out of phase, and represent the electronic states of the crystal. These modes introduce a local time-dependent polarization into the lattice. The lower-energy portion of this set of excitations is identified with plasmon²⁶ excitations, and the known properties of plasmons in germanium are utilized in the description of these states. The ordinary phonons will be referred to as the phonon modes while the modes with core and shell moving out of phase will be referred to as polarization modes.

In the above model it has been implicitly assumed that the energy losses of an ion channeling through a crystal are predominantly to the collective modes of the solid. This assumption is justified by reference to the energy-loss calculations of Bohr²⁷ who showed that in an amorphous solid the "distant resonant energy transfers" and the "close impact-type collisions" share equally in the energy lost by a fast incident particle. In the channeling situation, the "distant" processes are as probable as in the amorphous solid, while the

"close" collisions are significantly reduced due to the small electronic density in the channels. The channeling energy losses are thus primarily through the "distant" processes.

Recent studies on the statistics of the energy-loss process indicate further that even the "close" collisions do not generally result in large momentum transfers to individual electrons, but also excite collective modes. In fact, for simple valence-electron solids (of which germanium is an example) it is believed that a fast incident particle dissipates the major portion of its energy in the production of plasmons, even in the normal (random) solid.²⁸ This would indicate that a large fraction of the "close" collisions result in plasmon excitation.²⁹ These ideas are reflected in the model presented above.

Transition probabilities are considered in Sec. II. Numerical calculations are presented in Sec. III where focusing properties of the model described above are discussed. Section IV is a discussion and summary of the paper.

II. TRANSITION PROBABILITIES

A. General

A plane-wave ion of mass M and charge ze is assumed incident on a single-crystal target. The internal dynamics of the crystal are described in terms of ordinary and polarization phonons as described above. The shells have a charge of $-Z_i e$ and a mass of $Z_i m$ while the nuclei have a charge of $+Z_i e$ and a mass M_n . Z_i is the effective number of electrons on the i th atom which contribute to the lattice polarization. The value of Z_i will be left unspecified until theory is compared with the experiment in Secs. III and IV. The mass of a single electron is m and e is the electronic charge. The incident ion interacts with the electronic shells and the atomic cores through a Coulomb interaction represented by the Hamiltonian H' .

The transition probability of interest is $W(\mathbf{K}, \Delta\omega)$, the probability that the incident ion undergoes a change of momentum $\hbar\mathbf{K}$, accompanied by a simultaneous change in energy $\hbar\Delta\omega$. A straightforward application of first-order time-dependent perturbation theory with

²³ C. A. Klein, J. Phys. Soc. Japan Suppl., **21**, 307 (1966).

²⁹ This is also in agreement with measurements of electron-energy loss to thin films of extremely pure germanium [C. J. Powell, Proc. Phys. Soc. (London) **76**, 593 (1960)] which show energy loss only to collective electron modes of the solid. The low-energy loss structure reported in recent electron-energy loss measurements [K. Zeppenfeld and H. Raether, Z. Physik **193**, 471 (1966)] as well as earlier optical measurements [H. R. Philipp and H. Ehrenreich, Phys. Rev. **129**, 1550 (1963)] probably reflect the presence of a surface layer of oxide. Powell also found such structure in samples with an oxide layer, but no such structure was observed for his high-purity samples. Weak losses to d -electron excitation were also observed by Powell in some elements, but such losses were too weak to be observed in germanium. It is felt that these losses can safely be neglected compared with the plasmon losses, especially for germanium.

²⁴ A preliminary account of some of this work has been given by D. K. Brice [Bull. Am. Phys. Soc. **10**, 719 (1965)] and D. K. Brice and A. R. Sattler [*ibid.* **11**, 177 (1966)].

²⁵ W. Cochran, Proc. Roy. Soc. (London) **A253**, 260 (1959).

²⁶ A. A. Maradudin, E. W. Montroll, and G. H. Weiss, in *Solid State Physics*, edited by F. Seitz and D. Turnbull (Academic Press Inc., New York, 1963), Suppl. 3.

²⁷ D. Pines, Rev. Mod. Phys. **28**, 184 (1956); Phys. Rev. **92**, 626 (1953), and references contained therein.

²⁸ N. Bohr, Kgl. Danske. Videnskab. Selskab, Mat. Fys. Medd. **18**, No. 8 (1948).

the appropriate thermal average over initial lattice states and sum over final lattice states yields, for this probability,³⁰

$$W(\mathbf{K}, \Delta\omega) = \frac{\rho}{\hbar\sigma} \int_{-\infty}^{\infty} \exp(i\tau\Delta\omega) \times \text{Tr}\{\exp(-\lambda H_L) H_K \exp(-\gamma H_L) H_K^\dagger\} d\tau, \quad (1)$$

where τ is the variable of integration with units of time and

$$\begin{aligned} \gamma &= i\tau/\hbar, \\ \lambda &= 1/kT - \gamma, \\ \sigma &= \text{Tr}\{\exp(-H_L/kT)\}, \end{aligned} \quad (2)$$

k is the Boltzmann constant, T is the absolute temperature, and H_L is the Hamiltonian which describes the internal dynamics of the crystal.

The operator H_K ($\mathbf{K} = \mathbf{k}' - \mathbf{k}$) is defined as the matrix element of the operator H' between the initial ion state, $\Psi_{\mathbf{k}}$, and the final state $\Psi_{\mathbf{k}'}$. The initial and final wave vectors for the ion are \mathbf{k} and \mathbf{k}' , respectively. The quantity ρ is the density per unit energy range of lattice states. This density refers to those states of the lattice which contribute to the energy loss (gain) of the incident ion, and may be different from the actual density of lattice states. This point will be discussed further when (1) is evaluated.

As a consequence of the model for the internal lattice dynamics used in the calculations, the Hamiltonian H_L can be written as

$$H_L = \sum_{p,q} \hbar\omega_{pq} a_{pq}^\dagger a_{pq}, \quad (3)$$

where a_{pq}^\dagger and a_{pq} are creation and annihilation operators for the p th mode of the lattice with wave vector \mathbf{q} .³¹ Both phonon and polarization modes are included in the sum in Eq. (3).

The interaction between the incident ion and the crystal is taken to be

$$H' = ze^2 \sum_i Z_i \{1/|\mathbf{r}_p - \mathbf{r}_{ni}| - 1/|\mathbf{r}_p - \mathbf{r}_{si}|\}, \quad (4)$$

where \mathbf{r}_p is the position vector for the incident ion, \mathbf{r}_{ni} is the position of the i th atomic core, and \mathbf{r}_{si} is the position of the i th electronic shell. The position of an electronic shell is considered as the center of charge for that shell.

Matrix elements H_K calculated using (4) are determined with ion wave functions normalized in a volume V , the volume of the crystal. At the end of the calculation, the crystal volume will be allowed to become infinite while the atomic density remains constant. The resultant transition probability will then represent a single ion interacting with an infinite crystal through (4).

³⁰ For a similar derivation concerning the Mössbauer effect see B. Kaufmann and H. J. Lipkin, Ann. Phys. (N.Y.) **18**, 294 (1962).

³¹ Vector notation will be suppressed when \mathbf{q} is used as a subscript. When not a subscript, q will represent the magnitude of \mathbf{q} .

Using (3) and (4) Eq. (1) becomes

$$W(\mathbf{K}, \Delta\omega) = A_1 \int_{-\infty}^{\infty} \exp(i\Delta\omega\tau) U(\tau) d\tau, \quad (5)$$

where

$$A_1 = (16\pi^2 z^2 e^4 \rho) / (V^2 K^4 \hbar),$$

and

$$U(\tau) = \sum_{ij} Z_i Z_j \{ \Lambda_1^{ij} + \Lambda_2^{ij} + \Lambda_3^{ij} + \Lambda_4^{ij} \} \times \exp(i\mathbf{K} \cdot \mathbf{R}_{ij}),$$

$$\Lambda_n^{ij} = \exp\left\{ - \sum_{\alpha\beta} K_\alpha K_\beta [C_{\alpha\alpha}(0, 0) \delta_{\alpha\beta} - C_{\alpha\beta}(\mathbf{R}_{ij}, \tau)] \right\},$$

$$C_{\alpha\beta}(\mathbf{R}_{ij}, \tau) = \sum_{qp} (M_{\alpha i} M_{\beta j})^{-1/2} (\hbar e_{qp}^{\alpha i} e_{qp}^{\beta j}) / (2\omega_{qp} N)$$

$$\times \{ \exp[i(\mathbf{q} \cdot \mathbf{R}_{ij} - \omega_{qp}\tau)] - X_{qp} \cos(\mathbf{q} \cdot \mathbf{R}_{ij} - \omega_{qp}\tau) \},$$

$$X_{qp} = 2 \{ \exp[(\hbar\omega_{qp}) / (kT)] - 1 \}^{-1}. \quad (6)$$

In expressions (5) and (6) the variable \mathbf{R}_{ij} is the equilibrium separation of the i th and j th atoms and the indices αi and βj refer to Cartesian components of the displacements of electronic shells or cores of the i th or j th atom from their equilibrium positions in the lattice. In the function Λ_1 both αi and βj refer to core displacements; in Λ_2 and Λ_3 they refer, respectively, to a core displacement and to an electronic-shell displacement. In Λ_4 , both αi and βj refer to electronic-shell displacements. $M_\alpha = M_n$ for nuclear displacements and $M_\alpha = Zm$ for electronic-shell displacements. N is the number of primitive unit cells in the volume V .

The function $C_{\alpha\beta}(\mathbf{R}, \tau)$ is the time-dependent displacement correlation function introduced by Glauber,³² which depends on the phonon field of the lattice. ω_{qp} is the frequency of the (\mathbf{q}, p) lattice mode, while \mathbf{e}_{qp}^i is the polarization vector for this mode at the i th atom. The sum over \mathbf{q} and p includes a sum over both the phonon and polarization modes.

B. Approximations

The difficulty in evaluating the transition probability arises from a lack of detailed knowledge about the internal modes of the crystal. Some reasonable approximations will allow one to continue with the evaluation of the transition probabilities, while reducing the complexity of the expressions involved.

The following four approximations will be made:

(1) The total transition probability is large enough that the natural linewidth of an individual transition is much larger than the spread of the phonon spectrum.

(2) The displacement of the atomic cores due to the presence of the polarization modes is negligible compared with the corresponding displacement of the electronic shells.

(3) The polarization-mode frequency spectrum will be replaced by an "average" frequency ω .

³² R. J. Glauber, Phys. Rev. **98**, 1692 (1955).

(4) The interference effects in the function $C_{\alpha\beta}(\mathbf{R}, \tau)$ will be ignored.

The first of these approximations will be justified when the total transition probability is evaluated. This approximation is equivalent to saying that the interaction between the ion and the polarization modes is much stronger than the interaction between the ion and the phonon modes. It is also equivalent to replacing $\exp(i\omega_{qp}\tau)$ by 1 for the phonon modes. Since the phonon spectrum is germanium has a width of $\approx 10^{13}$ /sec, this requires that $W_T = \sum_{\Delta\omega, \mathbf{K}} W(\mathbf{K}, \Delta\omega)$ satisfy $W_T \gg 10^{13}$ /sec.

The second approximation is justified using the orthonormality relations for the lattice-mode polarization vectors \mathbf{e}_{qp} for fixed \mathbf{q} . Since phonons correspond to cases in which the electronic shell and the corresponding atomic core move as a unit while the shell and core move out of phase in the polarization modes, one obtains for the polarization-mode displacements x_{rms} (atomic core) $\approx (Zm/M_n)x_{\text{rms}}$ (electronic shell). The mass ratio is less than 1/4000 for most atomic systems.

The third approximation can be justified through the experimental measurements of the plasmon spectrum in germanium.³³ Averaging the energy of this spectrum over a spherical Brillouin zone one obtains as the average polarization-mode energy $\epsilon = 20.0$ eV. The rms deviation from this average is 1.6 eV. The curvature of the Ge spectrum is almost twice that measured for other materials; thus the use of approximation (3) for such materials should be even more accurate than it is for germanium. Approximation (3) will be used in the description of the polarization modes in germanium.³⁴

The fourth approximation is justified by invoking anharmonic forces in the lattice. These forces will cause both the phonon modes and the polarization modes to scatter, thus destroying any long-range correlations. In addition, the polarization modes should decay into lower-energy excitations of the lattice, further reducing their space correlations. The sums over i and j in Eqs. (5) and (6) extend over the entire lattice; thus most of the terms in that sum correspond to values of \mathbf{R}_{ij} for which correlations may be neglected. The factor $\exp(i\mathbf{q}\cdot\mathbf{R})$ will thus be replaced by unity in the correlation function $C_{\alpha\beta}$.

Approximations (1) and (2) eliminate the τ dependence of Λ_1^{ij} , Λ_2^{ij} , and Λ_3^{ij} . Similarly, approximations (3) and (4) eliminate the τ dependence in Λ_4^{ij} when i and j refer to inequivalent sites in the primitive unit cell because of the orthonormality of the polarization vectors \mathbf{e}_{qp} . Transition probabilities for events in which

the ion-exchanges energy with the lattice will depend only on those terms which have a τ dependence; thus other terms will be ignored in the following development. These terms would be of interest, however, in determining the magnitude of a "zero-phonon" line in experiments for which little energy transfer was expected between an incident ion and the lattice (e.g., transmission of ions through very thin films).

Retaining in $U(\tau)$ only those terms which have a τ dependence then yields for this function

$$U(\tau) = \sum'_{ij} Z_i^2 \exp(i\mathbf{K}\cdot\mathbf{R}_{ij}) \times \exp\{-g_i(K)[(1+r)/(1-r) - (1-r)^{-1} (\exp(-i\omega\tau) + r \exp(i\omega\tau))]\}, \quad (7)$$

where

$$g_i(\mathbf{K}) = (\hbar K^2)/(2Z_i m \omega), \quad (8)$$

$$r = \exp(-\hbar\omega/kT),$$

and the primed sum indicates a sum only over those i and j which refer to equivalent primitive-cell sites. Placing this expression for $U(\tau)$ in Eq. (5) yields

$$W(\mathbf{K}, \Delta\omega) = A \sum_i w_i(\mathbf{K}, n),$$

$$w_i(\mathbf{K}, n) = [g_i(\mathbf{K})]^{-2} r^{-n/2} I_n \left[\frac{2r^{1/2} g_i(\mathbf{K})}{1-r} \right] \times \exp \left[-g_i(\mathbf{K}) \left(\frac{1+r}{1-r} \right) \right], \quad (9)$$

where $I_n(y)$ is the hyperbolic Bessel function of order n and the sum over i is over the inequivalent sites in the primitive unit cell.

$$A = (8\pi^3 z^2 e^4 \hbar^3 N^2 \rho)/(m^2 \epsilon^2 V^2),$$

and from Eqs. (5) and (7) \mathbf{K} and $\Delta\omega$ are, respectively, restricted to values satisfying: \mathbf{K} = reciprocal lattice vector,

$$\hbar\Delta\omega = n\hbar\omega. \quad (10)$$

The selection rule on energy [Eq. (10)] arises because of the integration over τ . The selection rule on the K vector arises from the sum over i and j . The K selection rule is not conservation of crystal momentum because the correlation effects have been ignored. This selection rule arises since the incident ion interacts with atoms located on lattice sites. The variable ϵ appearing in the constant A is the average polarization-mode energy ($\epsilon = \hbar\omega$).

Since $\epsilon = 20.0$ eV for germanium, the temperature-dependent variable r will be negligible even for temperatures as high as the melting temperature of germanium (958°C). This will also be true of most other materials since the lower edge of the plasmon spectrum is generally in the range 10–20 eV. Transition probabilities, and other quantities derived from them (e.g., the stopping power), will thus be relatively insensitive to the temperature. The approximations (1) through (4) have allowed certain terms to be ignored in the prob-

³³ H. Watanabe, J. Phys. Soc. Japan 11, 112 (1956).

³⁴ The argument for using an effective Einstein spectrum in the description of the plasmons is further strengthened by the very weak dependence of the channeling stopping power on the plasmon energy. For example, for 8-MeV protons incident along $\langle 110 \rangle$ with $Z=5$ and $\epsilon=15$ eV one obtains $|dE/dx| = 52.10$ MeV/cm. This should be compared with the result of 50.53 MeV/cm obtained using $\epsilon=20$ eV (see Table I), a difference of only 3%.

ability expressions, however, which also depend upon temperature. These have been argued to be small. Since r is so extremely small in the temperature ranges of interest, it is quite likely that any small temperature dependence which might be observed would be due to the neglected terms rather than the temperature dependence indicated in Eq. (9). The quantity r will thus be set to zero which yields for the second of Eqs. (9)

$$w_i(\mathbf{K}, n) = (1/n!) \{g_i(\mathbf{K})\}^{n-2} \exp[-g_i(\mathbf{K})]. \quad (11)$$

Expression (11), multiplied by A , and summed over i , gives the desired transition probability for the creation of n polarization-mode quanta (plasmons) of energy ϵ accompanied by a change in incident-ion wave vector of \mathbf{K} . The sum over i is a sum over inequivalent sites in the primitive unit cell.

III. NUMERICAL CALCULATIONS

A. Energy Uncertainties

As indicated in Sec. IIB, in order for approximation (1) to be valid, the total transition probability through the polarization modes must be greater than 10^{13} /sec. When total transition probabilities are evaluated using Eqs. (9)–(11) one obtains transition probabilities of the order of 10^{16} to 10^{17} /sec. These large transition rates justify the use of approximation (1) in the calculations, but they require that one also take into account the energy uncertainties which will be introduced by the short transition times. A straightforward application of the theory of line-breadth phenomena³⁵ then yields a factor of

$$\frac{1}{2\pi} \frac{\Gamma}{\Gamma^2/4 + (E - E_0)^2} \quad (12)$$

which must multiply the transition probability for each transition. In (12) Γ is given by $\hbar W_T$. The total probability for a given transition is then obtained by integrating (summing for a discrete spectrum) over the values of E . The total transition probability to any state is then obtained by summing these "broadened" probabilities over all transitions allowed by the selection rules.

The stopping powers and differential mean-square energy spread of the channeling spectrum have been calculated using the "broadened" probabilities as described above. The focusing of channelled particles is discussed in the next subsection qualitatively, and the "broadened" probabilities have not been used there since the qualitative properties of the interaction are not changed by the broadening.³⁶

³⁵ V. Weisskopf and E. Wigner, *Z. Physik* **63**, 54 (1930); E. Arnow and W. Heitler, *Proc. Roy. Soc. (London)* **A220**, (1953).

³⁶ Use of the broadened probabilities greatly extends the running time of the computer program. The qualitative aspects of the predicted channeling phenomena are not altered by use of the unbroadened probabilities. The unbroadened probabilities are thus used when a numerical calculation would call for a prohibitive amount of computer time, but when it was desirable to illustrate the qualitative aspects of the interaction.

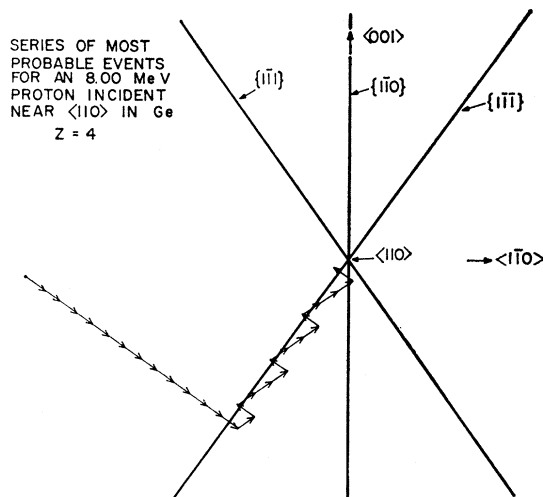


FIG. 1. Polar projection of a series of the most probable changes in the momentum of an 8-MeV proton incident on a germanium lattice. The pole of the projection is the $[110]$ crystallographic axis. The polar angle of the initial direction of incidence is 5×10^{-4} radians. These momentum changes were determined using the "unbroadened" probability function.

B. Planar and Axial Focusing

The focusing properties of the lattice for channelled particles have been investigated in the following way. A particle of given mass and energy was assumed incident near some crystallographic axis. The most probable transition was then determined using Eqs. (9)–(11). The momentum and energy of the incident ion were changed accordingly and the process repeated. The result of a set of such calculations is shown in Fig. 1. This figure shows a projection onto the $(1, 1, 0)$ plane of the changes in momentum for an 8-MeV proton initially incident near the $[1, 1, 0]$ direction.

One sees that the proton is first deflected toward the $(1, 1, 1)$ plane, the most open plane intersecting the $[1, 1, 0]$ axis. Similar calculations for initial proton momentum near other low-index crystallographic directions indicate that the most probable first deflections are always those which carry the momentum vector into the most open plane intersecting that direction. After reaching the most open plane, the momentum vector in Fig. 1 is then further deflected into the axial channel. The transitions which carry the momentum vector away from the plane or axis are, however, almost as probable as those which carry it toward the axis when the broadened probabilities are considered. The tendency toward axial and planar focusing, while real, is thus not as strong as one would expect from calculations made with the unbroadened probabilities.

One should note that this focusing mechanism does not depend upon direct collisions between the incident ion and the channel walls. Two features of the model, the long-range Coulomb potential and the plane-wave nature of the incident ion, are responsible for the focusing mechanism. The Coulomb potential provides an interaction between an atom at a lattice site and the

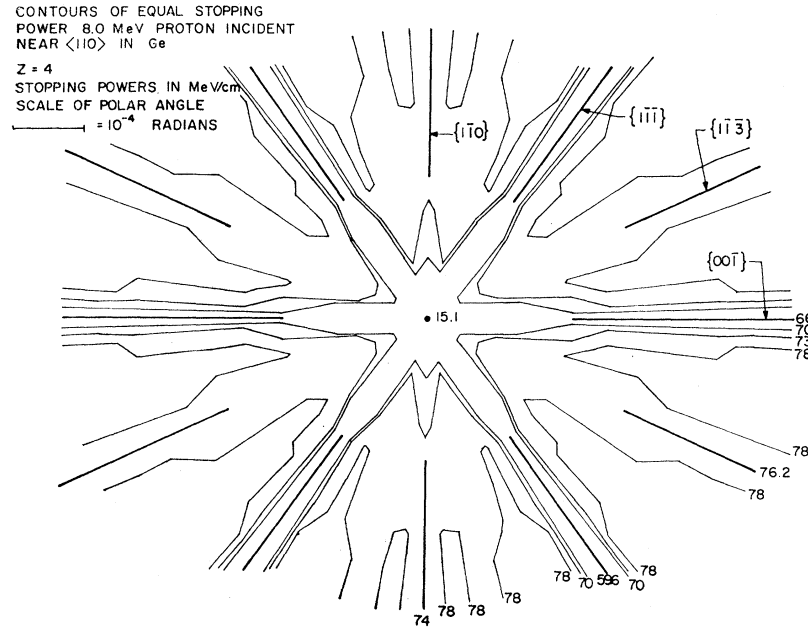


FIG. 2. Polar projection of the contours of equal stopping power for an 8-MeV proton incident near the $[110]$ crystallographic axis. The pole of the projection is the $[110]$ crystallographic axis. The scale of the polar angle for this projection is shown. These contours were determined using the "unbroadened" probability function.

incident ion even when they are widely separated and leads to the form of the probability function, $W(\mathbf{K}, n)$. The plane-wave nature of the incident ion leads to interference effects between the wave fronts scattered from different lattice sites and yields the selection rule on \mathbf{K} . This is analogous to the Bragg condition for the scattering of x rays from a crystal. The form of the probability function and the selection rule on \mathbf{K} together determine the focusing properties of the interactions. This, however, should not be taken to exclude other forms of focusing for ions which do interact with the "channel" through direct collisions with the walls.

C. Stopping Power

To determine the stopping power, one must evaluate the expression

$$-dE/dx = v^{-1} \sum_{\mathbf{K}} n\epsilon W(\mathbf{K}, n) \\ = (A/v) \sum_{\mathbf{i}} \sum_{\mathbf{K}} n\epsilon w_{\mathbf{i}}(\mathbf{K}, n), \quad (13)$$

where v is the ion speed. For ion and polarization-mode energies of interest, the probability function $W(\mathbf{K}, n)$ varies rapidly in some directions in wave-vector space in comparison with the spacing of the reciprocal lattice points. It is thus not appropriate in general to replace the summation in Eq. (13) by an integration. A general evaluation of the stopping power is then a formidable task even with the use of a high-speed computer. In certain cases of specific interest, however, the stopping power may be evaluated. These cases correspond to ions incident near major crystallographic directions. Before evaluating the stopping power for these cases some of the properties of the probability function $W(\mathbf{K}, n)$ should be pointed out.

For fixed n , the probability function $w_{\mathbf{i}}(\mathbf{K}, n)$ has a sharp maximum when $g_{\mathbf{i}}(\mathbf{K}) = n - 2$. The locus of such points forms a circle in \mathbf{K} space. The locus of such circles for variable n forms a spherical shell (which shall be referred to as the sphere of maximum probability) with a center located at $-(\mathbf{k}b)/(1+b)$. (\mathbf{k} is the incident proton wave vector and $b = Z_i/M$.) The diameter of the shell is given by

$$D = \frac{2kb}{(1+b)} \left\{ 1 - \frac{2(1+b)\epsilon}{Eb} \right\}^{1/2} \approx \frac{2kb}{(1+b)}. \quad (14)$$

Points on the shell in \mathbf{K} space nearer the origin correspond to higher probabilities. The complete set of points in \mathbf{K} space corresponding to a constant n also forms a spherical shell with center at $-\mathbf{k}$ and radius $k' = [k^2 - (2n\epsilon M)/\hbar^2]^{1/2}$, where \mathbf{k}' is the proton wave vector in the final state. Since $b \ll 1$, the spheres of constant n may be replaced by planes in the vicinity of the sphere of maximum probability.

The magnitude of the energy loss of protons incident normal to a set of planes of reciprocal lattice points may now be easily evaluated since the sum over \mathbf{K} in Eq. (13) is simplified. Each plane of reciprocal-lattice points can be characterized by a particular value of n in this case, and the sum can be done in two steps. First, the sum within a particular plane is done with constant n , and then the summation over n completes the evaluation.

A similar evaluation is possible for ions which are incident near a major crystallographic direction. In that case, a small angle approximation can be used and the sum evaluated as before. In both cases it is necessary to use a computer in the calculations.

Contours of equal stopping power have been determined for 8.0-MeV protons incident near the $[1, 1, 0]$

axis in germanium using the unbroadened probabilities.³⁶ The results of this calculation are shown in Fig. 2. The value of Z used in this determination is 4, the number of valence electrons per atom. As indicated earlier, the value of Z which will best explain the experimental data is expected to be $\gtrsim 4$. One notes in the figure that the contours of equal stopping power reproduce the starlike pattern of low-index planes which intersect at the $[1, 1, 0]$ axis. The stopping powers are relatively constant in the planes, but drop to a very small value along the axial channel.

The focusing properties discussed in the previous subsection indicate that the particles incident near a channeling axis will be deflected into one of the open planes intersecting that axis. The pattern of the emergent channelled particle beam is then predicted to re-

TABLE I. Calculated stopping power for protons in germanium.

Incident direction	Incident energy (MeV)	Stopping power (MeV/cm)	
$\langle 110 \rangle$		$Z=5$	$Z=6$
	8.0	50.53	59.44
	7.0	55.54	65.31
	6.0	61.75	72.83
	5.0	69.97	82.87
	4.0	81.77	97.24
	3.0	100.66	120.12
$\langle 112 \rangle$		$Z=7$	$Z=8$
	8.0	51.65	64.06
	7.0	57.65	71.24
	6.0	65.19	80.26
	5.0	75.85	92.95
	4.0	91.87	111.94
	3.0	116.26	140.83
$\langle 111 \rangle$		$Z=8$	$Z=9$
	8.0	56.13	66.65
	7.0	63.69	75.48
	6.0	72.11	85.34
	5.0	84.61	99.96
	4.0	104.56	123.21
	3.0	131.23	154.34

produce the star-shaped pattern seen in Fig. 2, and such has been observed experimentally.^{5,9} The present calculations thus show that a diffraction picture can successfully account for the observed patterns which are characteristic of the crystal geometry in the vicinity of a channeling axis.

If the "broadened" probabilities are used in producing Fig. 2, the essential features of the contours are reproduced. The significant differences in that case are that the stopping powers for a given value of Z are reduced, the anisotropy of the stopping power is greatly reduced, and the stopping power for ions incident down the axial direction is not appreciably different from that in the off-axis directions.³⁷ In addition, the axial

³⁷ For example, with 7.0-MeV protons, and $Z=5$ one obtains a stopping power of 55.54 MeV/cm down the $[110]$ axial direction, while at an angle of 0.01 radians from this direction in the (111) plane one obtains a value of 56.66 MeV/cm for the stopping power.

TABLE II. Calculated stopping power for deuterons in germanium.

Incident direction	Incident energy (MeV)	Stopping power (MeV/cm)	
$\langle 110 \rangle$		$Z=5$	$Z=6$
	8.0	81.74	97.13
	7.0	89.98	107.16
	6.0	101.17	120.81
	5.0	115.38	138.18
	4.0	135.00	162.15
	3.0	169.97	205.09
$\langle 112 \rangle$		$Z=7$	$Z=8$
	8.0	90.83	110.76
	7.0	102.38	124.40
	6.0	117.12	141.77
	5.0	137.90	166.20
	4.0	168.52	202.12
	3.0	212.39	253.64
$\langle 111 \rangle$		$Z=8$	$Z=9$
	8.0	105.36	124.39
	7.0	117.25	137.34
	6.0	138.04	157.81
	5.0	162.51	187.62
	4.0	192.11	232.52
	3.0	264.51	311.88

channel becomes broader, extending out to ~ 0.001 rad rather than the 0.0001 rad indicated.

Stopping powers have been calculated (using the "broadened" probabilities) for ${}^1\text{H}^+$, ${}^2\text{D}^+$, and ${}^3\text{He}^{++}$ for incidence near three major crystal axes in germanium and for energies in the range 3–8 MeV. These stopping powers are listed in Table I for ${}^1\text{H}^+$, Table II for ${}^2\text{D}^+$, and Table III for ${}^3\text{He}^{++}$ for two different values of Z for each direction. These values of Z are

TABLE III. Calculated stopping power for ${}^3\text{He}^{++}$ in germanium.

Incident direction	Incident energy (MeV)	Stopping power (MeV/cm)	
$\langle 110 \rangle$		$Z=5$	$Z=6$
	8.0	348.11	398.70
	7.0	389.66	445.94
	6.0	438.81	502.18
	5.0	504.24	577.18
	4.0	599.69	686.19
	3.0	748.89	854.59
$\langle 112 \rangle$		$Z=7$	$Z=8$
	8.0	566.04	650.07
	7.0	626.53	720.55
	6.0	716.84	824.52
	5.0	849.74	975.26
	4.0	1040.0	1189.8
	3.0	1289.1	1479.1
$\langle 111 \rangle$		$Z=8$	$Z=9$
	8.0	638.42	716.30
	7.0	713.11	801.15
	6.0	839.37	933.57
	5.0	989.64	1095.4
	4.0	1167.1	1296.7
	3.0	1543.6	1686.0

TABLE IV. Comparison of theoretical and experimental energy loss protons and deuterons in germanium.

Incident direction	Crystal thickness (10^{-3} cm)	Incident Ion	Incident* energy (MeV)	Energy loss (MeV)		Z
				Expt.	Theory	
$\langle 110 \rangle$	15.31	H^+	7.59	0.97 ± 0.05	0.929	5.6 ± 0.3
			7.07	1.00	0.983	
			6.57	1.01	1.042	
			6.10	1.08	1.107	
			5.54	1.14	1.202	
			5.05	1.25	1.306	
			4.54	1.44	1.447	
			4.03	1.71	1.647	
			7.35	1.60 ± 0.08	1.621	
			$\langle 112 \rangle$	12.80	H^+	
7.28	1.43 ± 0.08	1.449				
D^+	6.78	1.56			1.567	
	6.78	1.56			1.567	
$\langle 111 \rangle$	12.16	H^+	6.57	1.02 ± 0.05	0.964	8.6 ± 0.4
		D^+	6.78	1.75 ± 0.08	1.869	

* From Ref. 10.

presented since the experimental data will indicate that the actual value of Z for each of these directions lies between the two values of Z for which results are presented.

For comparison with experimental data the stopping powers can be integrated over a given path length (crystal thickness) and the predicted energy losses compared directly with the observed energy losses. This procedure has been carried out and is presented in Fig. 3 for protons incident near the $[1, 1, 0]$ direction in germanium and in Fig. 4 for deuterons incident near the $[1, 1, 0]$ direction. The data presented in these two figures are from Sattler and Dearnaly.¹⁰ No experimental data are presently available for $^3\text{He}^{++}$. These calculations along with those for the other direc-

tions are compared with experiment and tabulated in Table IV.

The best value of Z for each of these three directions has been obtained by using a linear interpolation between the Z values for which stopping powers are presented and making a least-mean-square-error fit to the experimental data. The results of this fit are

$$\begin{aligned} Z\langle 1, 1, 0 \rangle &= 5.6 \pm 0.3, \\ Z\langle 1, 1, 2 \rangle &= 7.2 \pm 0.3, \\ Z\langle 1, 1, 1 \rangle &= 8.6 \pm 0.4. \end{aligned} \quad (15)$$

These values of Z represent the effective number of electrons per atom which participate in the shell motion

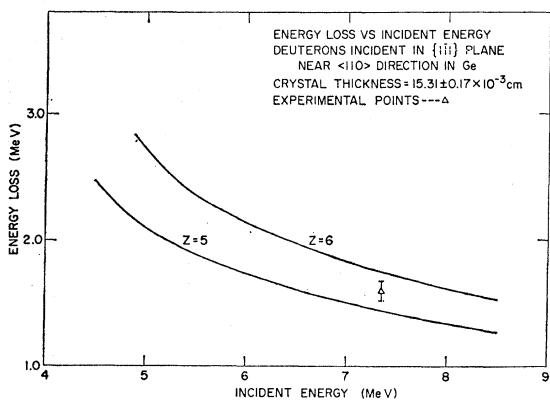


FIG. 3. Energy loss versus incident energy for protons incident in the $\langle 111 \rangle$ plane near the $[110]$ crystallographic axis of germanium. Curves are calculated as indicated in the text. Experimental points from Ref. 10 are shown.

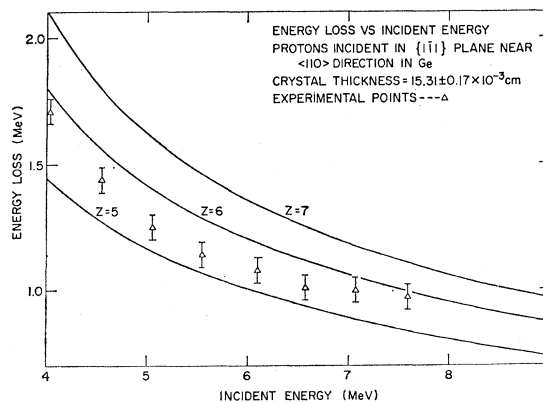


FIG. 4. Energy loss versus incident energy for deuterons incident in the $\langle 111 \rangle$ plane near the $[110]$ crystallographic axis in germanium. Curves show calculated values. Experimental points are from Ref. 10.

when ions are incident in the directions indicated. That the value of Z is anisotropic should not be too surprising since the channels are of different size in the various directions and the ion will on the average pass closer to the atoms in the more constricted channels. The inner electrons on the atoms are thus less effectively shielded and can participate more strongly in the interaction.

If the atoms in a zinc-blende type lattice are assumed to be spheres of radii equal to half the nearest-neighbor distance, then the rms distance of closest approach to the atomic centers for ions channeling down the various axes is

$$\begin{aligned} R_{\text{rms}}\langle 1, 1, 0 \rangle &= 0.269a_0, \\ R_{\text{rms}}\langle 1, 1, 2 \rangle &= 0.236a_0, \\ R_{\text{rms}}\langle 1, 1, 1 \rangle &= 0.223a_0, \end{aligned} \quad (16)$$

where a_0 is the lattice constant for the material. In comparing (15) and (16) one can easily see that the larger values of Z correlate with the smaller values of R_{rms} .

D. Straggling

The straggling of the particles can also be determined by the same sort of calculation which yields the stopping power. To determine the straggling or mean-square spread in energy of the transmitted beam of channeled particles it is necessary to calculate (as a function of ion energy) the zeroth, first, and second energy moments of the probability distribution given in Eq. (9). Let M_k be the k th energy moment of the probability distribution defined by

$$M_k = \sum_{\mathbf{K}} (\Delta E)^k W(\mathbf{K}, n), \quad (17)$$

where ΔE is given by Eq. (10). Also, let the k th energy moment of the spectrum of the transmitted beam of channeled particles be defined by

$$E_k = \int E^k G(E) dE, \quad (18)$$

where $G(E)$ is the energy spectrum of the channeled beam. The mean-square energy spread of this spectrum is then given by $\sigma^2 = E_2/E_0 - (E_1/E_0)^2$. The relation of σ^2 to the energy moments of the probability distribution is obtained through

$$\begin{aligned} \sigma^2 &= \sum_{\text{events}} \{M_2/M_0 - (M_1/M_0)^2\} \\ &= \int_0^{N'} \{M_2/M_0 - (M_1/M_0)^2\} dN', \end{aligned} \quad (19)$$

where N' represents the average number of scattering events a channeled particle undergoes in traversing

TABLE V. $d\sigma^2/dE$ for ${}^1\text{H}^+$, ${}^2\text{D}^+$ and ${}^3\text{He}^{++}$ incident on a germanium lattice.

Incident direction	Z^a	Energy (MeV)	$-d\sigma^2/dE \times 10^3$ (MeV ² /MeV)		
			${}^1\text{H}^+$	${}^2\text{D}^+$	${}^3\text{He}^{++}$
$\langle 110 \rangle$	5.6	8.0	6.5	4.0	3.8
		7.0	5.9	3.6	3.4
		6.0	5.3	3.2	3.0
		5.0	4.6	2.8	2.6
		4.0	4.0	2.4	2.2
		3.0	3.2	1.9	1.7
$\langle 112 \rangle$	7.2	8.0	11.1	6.3	4.1
		7.0	9.9	5.6	3.7
		6.0	8.8	4.9	3.2
		5.0	7.5	4.2	2.7
		4.0	6.2	3.4	2.2
		3.0	4.9	2.7	1.8
$\langle 111 \rangle$	8.6	8.0	13.6	7.3	5.0
		7.0	12.0	6.6	4.4
		6.0	10.6	5.7	3.8
		5.0	9.1	4.8	3.2
		4.0	7.4	3.9	2.7
		3.0	5.9	2.9	2.1

^a Least-mean-square error value from comparison of theoretical and experimental stopping power.

the crystal. The average energy loss per dN' events is given by dE , where $dE = -(M_1/M_0)dN'$. Thus the last of Eqs. (19) can be written

$$\sigma^2 = - \int (M_2/M_1 - M_1/M_0) dE, \quad (20)$$

or, in differential form,

$$d\sigma^2/dE = -(M_2/M_1 - M_1/M_0). \quad (21)$$

The moments M_0 , M_1 , and M_2 have been calculated according to Eq. (17) and combined in the form given in Eq. (21) to obtain $d\sigma^2/dE$. Because the contributions to the probability function from Λ_1 , Λ_2 , and Λ_3 [see Eqs. (5) and (6)] have been neglected, M_0 is in error by the zero-energy transfer probability contribution of these functions. The quantities M_1 and M_2 are correctly given by (17), however. The calculated values of the moments M_k indicate that M_2/M_1 is much larger than M_1/M_0 . Thus changes in M_0 by as much as an order of magnitude would affect the value of $d\sigma^2/dE$ by no more than 5–10%. It is expected that the zero-energy transfer events will not be 10 times as probable as all other events combined, but that they will be about equally probable with all other events. The calculated values of $d\sigma^2/dE$ should be in error by no more than 1–2%.

The calculated values for $d\sigma^2/dE$ are tabulated in Table V for the values of Z given in the expressions

(15). The observed channeling spectrum of Sattler and Dearnaley¹⁰ is not sufficiently collimated to permit a numerical comparison between the experimental and theoretical values of σ^2 . That is, many of the particles appearing in the low-energy loss spectrum presented in Ref. 10 are particles which were marginally channeled and did not remain in the channeling beam either because of interactions with lattice defects, the channel walls, or through other processes. These particles were accepted in the channeling spectrum because of the large acceptance aperture used in the experiments.

A qualitative comparison can be obtained by noting that the experimental channeling peak (if highly collimated) should have a width less than that observed. The experimental width is about $\sigma \simeq 0.22$ MeV for the spectrum shown in Ref. 10 for 6.57-MeV protons incident along the $\langle 1, 1, 0 \rangle$ axis.³⁸ From Table V and Eq. (20) one obtains for this case $\sigma \simeq 0.086$ MeV. Thus the calculated straggling is in reasonable agreement with the experimental data. Experiments in which a higher degree of collimation is used, such as those of Gibson *et al.* in Si,¹¹ yield much narrower channeling peaks with normal energy-loss peaks greatly reduced in relative intensity. No such data are presently available for germanium.

IV. CONCLUSION

Tables of the stopping power and the differential mean-square energy spread have been calculated for $^1H^+$, $^2D^+$, and $^3He^+$ ions channeling in a germanium lattice. The calculation utilizes a diffraction picture through the use of plane waves to represent the incident ion. The lattice polarization is represented through a shell model of the lattice atoms.

The effective number of electrons per atom which participate in the interaction with the channeling ion is found to be a function of the incident-ion direction. It is further noted that the closer the average distance of approach the channeling ion makes to the channel walls, the larger the effective number of electrons which participate in the interaction.

The effective number of electrons per atom participating in the interaction between the lattice and channeled protons and deuterons in germanium has been obtained by Erginsoy *et al.*,³⁹ who compare the observed and calculated straggling using a classical picture of the channeling ion. In those calculations the effective number of electrons per atom participating in the interaction is also a function of direction with Z values of slightly less than 6 for channeling in a $\{1, 1, 1\}$ planar channel and slightly greater than 6 for channeling in a $\{1, 1, 0\}$ planar channel being obtained.

³⁸ This corresponds to the third entry of Table IV.

³⁹ C. Erginsoy, B. R. Appleton, and W. M. Gibson, *Bull. Am. Phys. Soc.* **11**, 176 (1966).

The values of Z obtained by the two methods are then in fair agreement. Use of a different potential (*e.g.*, the Bohr potential) or a different model for the lattice polarization would yield slightly different values of the parameter Z . Variations in this parameter should thus be expected when calculations are carried out using different models. The present paper has shown, however, that the stopping power can be calculated from a diffraction picture using reasonable values of the parameter Z . In addition, the straggling is predicted within the experimental uncertainty for the same value of Z . A more accurate comparison of theory and experiment will require experimental data obtained with the incident- and emergent-particle beams collimated to within several hundredths of a degree.

The present calculation has also shown that the temperature dependence of the stopping power and differential mean square energy spread is quite small. Although no data are available for channeling in germanium, experimental measurements of the temperature dependence have been reported by Thompson *et al.*⁴⁰ for protons channeling in copper. They find that the channeling fraction decreases with increasing temperature, but no changes are observed in the energy losses. This is in agreement with the predictions of this paper.

The same calculational techniques which have been used in the present paper to describe the interactions between a target crystal and a channeling particle should also be applicable to a wide variety of incident particles over a broad range of incident energies. The energy range should be restricted from above by the nonrelativistic nature of the calculations, and from below by the requirement that electronic excitations in the target be the major source of energy loss. While there is no clear low-energy cutoff for this region the method should apply as long as the velocity of the incident particle is large compared with the velocity of the outer electrons of the target atoms. One should also be able to describe the channeling of heavier and lighter particles although some of the explicit approximations used in the present paper may require alteration. In addition, for very heavy particles electron exchange may occur between the target and the channeling particle, in which case the simple Coulomb potential used here would no longer adequately describe the interaction.

ACKNOWLEDGMENTS

I would like to express my appreciation to F. L. Vook, A. R. Sattler, and T. A. Green, all of Sandia Laboratory, for their helpful discussion of the ideas presented here.

⁴⁰ M. W. Thompson, R. S. Nelson, and R. Sizmann, in *Proceedings of the International Conference on Electron Diffraction and Crystal Defects, Melbourne, 1965* (Pergamon Press Inc., New York, 1966), II B-4.